

Low-loss, wide-angle Y splitter at $\sim 1.6\text{-}\mu\text{m}$ wavelengths built with a two-dimensional photonic crystal

S. Y. Lin, E. Chow, and J. Bur

MS 0603, Sandia National Laboratories, P.O. Box 5800, Albuquerque, New Mexico 87185

S. G. Johnson and J. D. Joannopoulos

Department of Physics, Massachusetts Institute of Technology, Cambridge, Massachusetts 02139

Received February 6, 2002

We report a successful experimental realization of a photonic-crystal Y splitter operating at $\lambda \sim 1.6 \mu\text{m}$. Our device has a large splitting angle of 120° and a miniature size of $\sim 3 \mu\text{m} \times 3 \mu\text{m}$. Furthermore, the Y-splitter loss is measured to be 0.5–1 dB at $\lambda = 1640\text{--}1680 \text{ nm}$, making the Y splitter promising for integrated photonic-circuit applications. These unique properties are attributed to the new guiding principle made possible by the photonic bandgap. © 2002 Optical Society of America

OCIS codes: 230.1360, 230.7370.

Among the most basic optical components for integrated optics applications are linear waveguides, waveguide bends, and Y splitters.¹ In the past few years, there have been many reports on the design, fabrication, and testing of two-dimensional (2D) photonic-crystal guides and bends.^{2–5} Quantitative analysis of guiding and bending efficiency at $\lambda = 1.5\text{--}1.6 \mu\text{m}$ wavelengths has also been carried out.^{3,4} It is demonstrated that a 2D photonic bandgap (PBG) is effective in light guiding and bending in the 2D plane. It is also possible to minimize radiation loss along the third direction by use of a strong-index cladding design.^{6–8} The same PBG guiding principle can also be applied to the design of a Y splitter with high efficiency. A PBG splitter can support large angle splitting ($>60^\circ$), is low loss, and also has a miniature size, $<5 \mu\text{m} \times 5 \mu\text{m}$. However, for a conventional waveguide branch (or Y splitter), the Y-splitting angle is restricted by radiation loss to a few (<10) degrees.^{9,10} Theoretical analysis of PBG splitters was performed recently for 2D photonic crystals.^{11–13} Experimental work on PBG Y splitters in the microwave regime is also just emerging.¹⁴ So far, to our knowledge, there has been no experimental analysis of either 2D or three-dimensional PBG Y splitters at the important communication wavelengths $\lambda = 1.5\text{--}1.6 \mu\text{m}$.

Here, we report what is believed to be the first quantitative analysis of a PBG Y splitter at $\lambda \sim 1.6 \mu\text{m}$, built on a 2D photonic crystal slab structure. Our device is based on a triple-line-defect design, has a Y-splitting angle of 120° , and a small size of $\sim 3 \mu\text{m} \times 3 \mu\text{m}$. The combined splitting and bending loss is measured to be ~ 0.5 dB, making this device promising for integrated photonic-circuit applications.

A scanning electron micrograph (SEM) of our Y splitter sample is shown in Fig. 1. Central to our design is a 120° Y splitter and two 60° bends. Light is guided by an input ridge waveguide, split into two by the Y splitter, bent, and then guided into two output ridge waveguides. Five linear PBG waveguides are used to connect the splitter, the bends, and the input–output ridge waveguides. The basic photonic-crystal structure is a 2D triangular hole

array, with lattice constant $a = 440 \text{ nm}$ and hole diameter $d = 0.6a = 264 \text{ nm}$. A previous measurement showed that such a photonic-crystal slab has a large TE-like (transverse electric) bandgap from $0.255 < \omega(a/\lambda) < 0.325$.⁷ The linear PBG waveguide consists of a triple line defect with a hole diameter $d' = 0.8a = 352 \text{ nm}$. The PBG guide is shown to have three guided modes.³ Note that the first even mode never overlaps other truly guided modes in frequency. Therefore, for $0.255 < \omega(a/\lambda) < 0.28$, the PBG guide supports only the first even mode.³ All PBG components used in this design are miniaturized. The Y splitter is $\sim 3 \mu\text{m} \times 3 \mu\text{m}$, the bend is $\sim 2 \mu\text{m} \times 2 \mu\text{m}$ and the whole sample is $\sim 10 \mu\text{m} \times 15 \mu\text{m}$.

Testing and analysis of the PBG Y splitter sample presents several experimental challenges. First, the input coupling of light must be precise, as the GaAs light-guiding layer is only 220 nm thick. A misalignment in the z direction [see Fig. 1(b) and the inset of Fig. 3(a), below] reduces the overall coupling efficiency, and a misalignment in the x direction affects both the coupling efficiency and the Y-splitting ratio.⁹ Second, the output intensity is affected by several loss mechanisms, which complicates our quantitative data analysis. The overall loss includes the Y-splitter radiation loss, the bending loss, the interfacial reflection losses, and the PBG guiding loss. Assuming that the Y splitter and the bends are not mutually interacting, the output may be written as $\text{output} = I_o(1 - R_1)P_1YP_2BP_3(1 - R_2)$. Here, I_o is the ridge-waveguide output intensity, R_1 and R_2 the interfacial reflection losses, P_1 , P_2 , and P_3 are the PBG guiding efficiency, B is the bending efficiency, and Y is the splitting efficiency. Note that the non-interacting picture is a good approximation only when the splitting, bending, and reflection losses are low.

To obtain a transmission spectrum, we use a high-resolution tunable diode laser. The laser beam is linearly polarized and focused into an input waveguide by a high-numerical-aperture microscope objective. The output light is split and then fed into an InGaAs photodetector for intensity measurement and an infrared camera for mode profile monitoring. This procedure

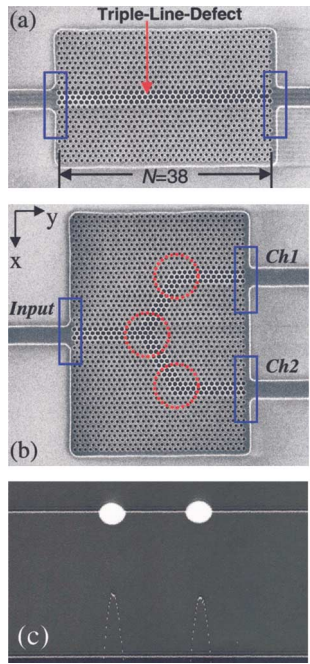


Fig. 1. (a) Scanning electron micrograph top view of 38 period ($N = 38$) triple-line-defect linear waveguide. The defect hole diameter is $d' = 0.8a = 352$ nm. The rectangular boxes indicate the interfaces between the ridge and the PBG waveguide. (b) Scanning electron micrograph image of the Y-splitter sample, which consists of a 120° Y-splitter and two 60° bends (indicated by the red circles). (c) Infrared camera image of the two Y-splitter outputs at $\lambda = 1650$ nm. They are both Gaussian-like and equally bright, indicating a near 50/50 splitting ratio.

ensures that the guiding mode signal but not the scattered leakage light is fed into the detector.

We first study an $N = 38$ PBG linear waveguide [Fig. 1(a)] to determine the interfacial reflection loss and the guiding loss. The PBG guiding output is given by $I_o(1 - R_1)P_1P_2P_3(1 - R_2)$. Figure 2 shows TE transmission spectra taken from a straight ridge waveguide (labeled Ridge WG) and a 38-period PBG waveguide (labeled $N = 38$). The spectra are plotted on a semi-log scale, and the units are the voltage output from an InGaAs photodetector. The inset shows the light output image, which has a Gaussian-like mode profile. The ridge-waveguide spectrum (the reference, I_o) is essentially λ independent and has an average intensity of 32 (solid line). The PBG waveguide spectrum, however, exhibits several strong dips with a period of $\Delta\lambda = 15 \pm 3$ nm. These dips are attributed to Fabry–Perot resonance between the two photonic-crystal–ridge-waveguide interfaces. From the known $\Delta\lambda$, λ , and photonic-crystal length ($L = 38$, $a = 16.7$ μm), one can deduce a corresponding k value of 1.44 ($2\pi/a$). This k value is shifted by ($k \pm 2\pi/a$) into the first Brillouin zone and becomes 0.44 ($2\pi/a$).¹⁵ The k value can also be obtained from the dispersion curve,³ which gives $\omega = a/\lambda = 0.267$ and $k = 0.41$ ($2\pi/a$). The agreement between experiment and theory is good. Except for the oscillations, the PBG guide spectrum displays a constant amplitude of 24 (dashed line) for $\lambda < 1675$ nm and drops

slightly for $1675 \text{ nm} < \lambda < 1685 \text{ nm}$. The intensity drop, from 32 to 24, or equivalently a 1.25-dB loss, is due to the combined reflection loss (R) and the guiding loss (P) for $N = 38$ periods. The reflection loss, R , can be determined from modal index of the ridge and photonic-crystal waveguides. The estimated reflection loss is $R \sim 10\%$, or 0.45 dB per interface, and the estimated guiding loss is $P \sim 0.35$ dB for $L = 16.7$ μm .

Next, we study the PBG Y-splitter device shown in Fig. 1(b). An image of the two Y-splitter outputs at $\lambda = 1650$ nm is shown in Fig. 1(c). They are both Gaussian-like and equally bright, indicating a near 50/50 splitting ratio. However, a good mode profile alone is not sufficient for obtaining a reliable splitting ratio and efficiency. Extra caution must be taken in the lateral alignment of the laser to the sample. In Fig. 3, both the Y-splitter outputs, Ch1 and Ch2, are plotted as a function of misalignment in the x axis, Δx . The Ch1 and Ch2 outputs remain equal for $\Delta x = -1$ μm to 1 μm and start to deviate from each other for larger Δx . For $\Delta x < 1$ μm , the total intensity (Ch1 + Ch2) has a maximum value of $\sim 22 \pm 2$. Compared with the $N = 38$ PBG guide output, 24 ± 2 , the overall Y-splitter loss is less than 0.5 dB at $\lambda = 1650$ nm. When the splitter, bends, and interfaces are not strongly interacting and their losses low, this loss value is a measure of the combined bending and splitting loss. The same measurement is repeated for misalignment in the z axis, i.e., up–down. In this case, the Y-splitter outputs are even more sensitive to z alignment. Still, the optimal intensity occurs near $\Delta z = 0$ and yields an ~ 0.5 -dB loss. Note that the intensities of Ch1 and Ch2 cross at $\Delta x = 1$ and -3 μm , suggesting an intensity redistribution between the two channels. Although the measured Y-splitter loss is low, other losses must also be minimized for a PBG splitter to be more efficient than the conventional ones.^{9,10} It is further noted that the intrinsic loss predicted for a threefold symmetry Y splitter such as ours is also ~ 0.5 dB.¹³ Compared with a conventional splitter, the splitting angle of 120° is an order of magnitude larger and the device size of 3 $\mu\text{m} \times 3$ μm is an order of magnitude more compact.

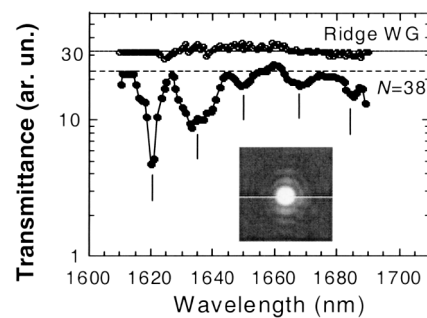


Fig. 2. Transmittance taken from a straight ridge waveguide (WG) and a linear $N = 38$ PBG waveguide. The ridge-waveguide spectrum is essentially λ independent (solid line) and is the reference. The PBG guide spectrum exhibits a constant amplitude (dashed line) with several equal spacing dips that are attributed to Fabry–Perot resonance. The inset shows the light output image.

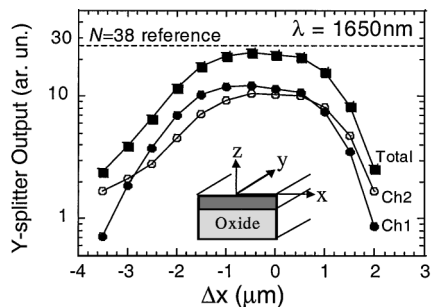


Fig. 3. Y-splitter output signals at $\lambda = 1650$ nm versus laser input misalignment, Δx . For small Δx (-1 to $1 \mu\text{m}$), the Ch1 and Ch2 intensities are nearly the same and the total intensity (Ch1 + Ch2) reaches its maximum value, 22 ± 2 . This value is $\sim 10\%$ less than that for the $N = 38$ reference and, therefore, the combined splitting and bending loss is less than 0.5 dB. The inset shows a schematic geometry of the input waveguide.

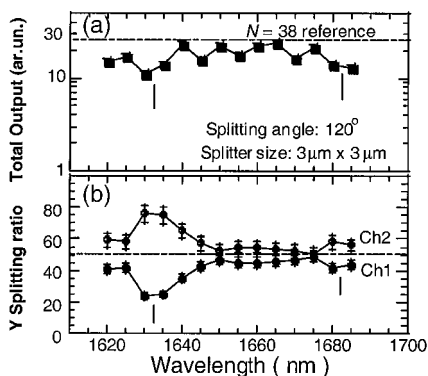


Fig. 4. Measured total output power and splitting ratio versus wavelength for $\lambda = 1620$ – 1685 nm. For $1640 \text{ nm} < \lambda < 1680 \text{ nm}$, the loss is low (~ 1 dB) and the splitting ratio remains even ($50 \pm 5\%$). However, for $\lambda < 1640$ nm and $\lambda > 1680$ nm, the loss is higher (>3 – 4 dB) and the splitting becomes uneven.

Finally, we examine the bandwidth aspect of our Y splitter by repeating the same measurement for $\lambda = 1620$ – 1685 nm. Figure 4 shows the measured total output power spectra and splitting ratio. For $1640 \text{ nm} < \lambda < 1680$ nm, the total output power approaches that for the $N = 38$ reference, and the loss is low (<1 dB). In Fig. 4(b), the measured splitting ratio is also roughly even ($50 \pm 5\%$) for the same λ range. For $\lambda < 1640$ nm and $\lambda > 1680$ nm, the splitting ratio becomes uneven and the total output power is also reduced. The origin of reduced total output power and uneven splitting ratio is not known at present. From symmetry consideration, the splitting ratio must be even for all λ . It is likely that the deviation of the Y-splitting ratio from 50% is caused by quasi-guided or resonant modes.⁹ As the biggest deviations come at frequencies where the $N = 38$ transmission spectrum has a sharp dip, suggesting a regime of resonant rather than guided modes.

The various losses occurred in our PBG splitter can be improved by use of new design schemes. First, the reflection loss (R) is due to the index mismatch at the

interface and can be reduced by improvement of the interfacial design. Second, the Y-splitter loss of 0.5 dB is intrinsic to the threefold symmetry of our Y-splitter design. By introduction of an intentional defect at the Y junction, the threefold symmetry is broken and better efficiency is expected.¹⁵ Third, structure disorder and symmetry breaking can both lead to PBG guiding loss. For an asymmetrical photonic-crystal slab, a TE–TM mode conversion can occur,⁴ which renders a PBG guide less effective. The mode conversion could also be reduced by use of a symmetrical 2D photonic-crystal slab geometry.

In summary, we report for the first successful experimental realization of a photonic-crystal Y splitter operating at $\lambda \sim 1.6 \mu\text{m}$. Our device has a large branching angle of 120° , a broad bandwidth, and a miniature size of $\sim 3 \mu\text{m} \times 3 \mu\text{m}$. The combined splitting and bending loss is measured to be ~ 0.5 dB at $\lambda \sim 1650$ nm, the theoretical limit set by the threefold symmetry of the Y splitter design.

The work at Sandia National Laboratories is supported through the U.S. Department of Energy. Sandia is a multiprogram laboratory operated by Sandia Corporation, a Lockheed Martin Company, for the United States Department of Energy under contract DE-AC04-94AL 85000. S.-Y. Lin's e-mail address is slin@sandia.gov.

References

1. See for example, C. Yeh, *Applied Photonics* (Academic, New York, 1990), Chap. 11.
2. S. Y. Lin, E. Chow, V. Hietala, P. R. Villeneuve, and J. D. Joannopoulos, *Science* **282**, 274 (1998).
3. S. Y. Lin, E. Chow, S. G. Johnson, and J. D. Joannopoulos, *Opt. Lett.* **25**, 1297 (2000).
4. E. Chow, S. Y. Lin, S. G. Johnson, and J. D. Joannopoulos, *Opt. Lett.* **26**, 286 (2001).
5. A. Talneau, L. Le Gouezigou, N. Bouadma, M. Kafesaki, C. M. Soukoulis, and M. Agio, *Appl. Phys. Lett.* **80**, 547 (2002).
6. P. R. Villeneuve, S. Fan, S. G. Johnson, and J. D. Joannopoulos, *IEEE Proc. Optoelectron.* **145**, 384 (1998).
7. E. Chow, S. Y. Lin, S. G. Johnson, P. R. Villeneuve, J. D. Joannopoulos, J. R. Wendt, G. A. Vawter, W. Zubrzycki, H. Hou, and A. Alleman, *Nature* **407**, 983 (2000).
8. S. G. Johnson, S. Fan, P. R. Villeneuve, J. D. Joannopoulos, and L. A. Kolodziejski, *Phys. Rev. B* **60**, 5751 (1999).
9. A. Klekamp, P. Kersten, and W. Rehm, *J. Lightwave Technol.* **14**, 2684 (1996).
10. H. Hatami-Hanza, M. J. Lederer, P. L. Chu, and I. M. Skinner, *J. Lightwave Technol.* **12**, 208 (1994).
11. T. Sondegaard and K. H. Dridi, *Phys. Rev. B* **61**, 15,688 (2000).
12. J. Yonekura, M. Ikeda, and T. Baba, *J. Lightwave Technol.* **17**, 1500 (1999).
13. S. Fan, S. G. Johnson, J. D. Joannopoulos, C. Manolatos, and H. A. Haus, *J. Opt. Soc. Am. B* **18**, 162 (2001).
14. M. Bayindir, B. Temelkuran, and E. Ozbay, *Appl. Phys. Lett.* **77**, 3907 (2000).
15. S. Fan, I. Applebaum, and J. D. Joannopoulos, *Appl. Phys. Lett.* **75**, 3461 (1991).